Modelling of Hull Lift and Cross Flow Drag Forces in Large Waves in a Computationally Efficient Dynamic Stability Prediction Tool

Michael J. Hughes, Paul J. Kopp and Ronald W Miller
David Taylor Model Basin (NSWC/CD)

ABSTRACT

The US Navy is developing a new computationally efficient simulation tool to predict the responses of a ship operating in severe sea states. The tool computes the total force on the ship as the summation of component forces. An important component to the total force on the ship is the force from hull lift and cross-flow separation. These forces are predicted in calm water by maneuvering simulation tools but are often ignored by traditional seakeeping simulation tools. As viscous effects are important in the prediction of these forces, most maneuvering simulations are based on empirical data from calm water maneuvering tests. While these methods are valid in calm water the wetted shape of the hull changes significantly in large waves having significant influences on the hull lift and cross flow drag forces. In the present method a hull lift and cross flow drag force model is presented that accounts for the varying wetted geometry of the hull in waves. The method uses calm water maneuvering data from model tests and RANS calculations to calibrate the model. Proper modeling of the hull lift and cross flow drag force in large waves is very important for the prediction of some dynamic stability events such as broaching and broaching leading to capsize.

KEYWORDS
Tempest, Maneuvering in Waves, CFD, Dynamic Stability.

INTRODUCTION

The US Navy is in the process of developing a new computational tool, called Tempest, for simulating the responses of a ship operating in severe sea states. An overview of this tool was provided in (Belknap 2010). Tempest computes the total force on the ship at each time step as a summation of component forces. An important component force is that from circulatory lift and cross-flow separation on the ship's hull. This force component is sometimes referred to as the hull maneuvering force, as it is predicted in calm water by maneuvering simulation tools but is often ignored by traditional seakeeping simulation tools. As Tempest will be applied to a ship maneuvering in large waves, the maneuvering force model should not rely purely on empirical coefficients obtained from calm water model tests. To the greatest extent possible, the method should model the physics of the problem and be geometry based, but with the ability to be "calibrated" for a specific ship based on known full-scale or model-scale maneuvering data. An additional requirement is that the model be well behaved within the context of a maneuvering-in-waves framework where the "seakeeping" forces are determined from potential flow assumptions (ideal fluid, no vorticity). Within this framework, there can potentially exist large heel and drift angles, as well as large sway and yaw rates. Furthermore, the maneuvering force/moment model needs to include the influence of the incident waves on the angle of attack of the ship hull relative to the local fluid velocity, though it must be consistent with an overall hydrodynamic model that does not provide the fluid velocity due to radiation and diffraction. The focus of this work is bare hull forces and moments since the rudder and propulsion forces are already included separately in Tempest, along with the wave induced seakeeping forces and moments, including, for example, added mass and slowly varying drift forces. As discussed in Belknap (2010) the theory in Tempest is being implemented in two phases. This paper describes the model that has been developed for the first phase. The second phase

of the hull lift and cross flow drag force implementation will apply the vortex-lattice techniques developed for the bilge-keel force model (Greeley 2011). The goal of the first phase model is to account for the time varying wetted geometry of the hull, while having the ability to tune the model to match available calm water maneuvering data. This method is expected to be faster and simpler than the model that will be implemented during the second phase. The first phase model is based partially on those of Ross (2008), Hooft (1994), and Hoerner (1965) and includes several modifications that are necessary to meet the requirements. Some example calculations are shown for the pre-contract DDG-51 hull form in calm water. This paper will present an overview of the model. A more detailed description can be found in Hughes (2011).

APPROACH OVERVIEW

The approach utilizes a blended model that is composed of two separate parts. The first treats the hull as a low aspect ratio airfoil in order to determine the normal force and moment on the ship due to circulatory lift. The other part of the overall approach is a cross-flow drag model that is based on an integrated 2D sectional analysis. Both portions account for the instantaneous submerged hull geometry in the presence of, potentially, large amplitude waves, orientation angles, and rotational/directional rates, while partially accounting for wave orbital velocities.

The normal force on the hull from circulatory lift and flow separation consists of a linear and quadratic term, expressed in the form of Eqn. (1), where β is the drift angle. It is assumed that the linear term represents the circulatory lift on the hull while the quadratic term represents cross-flow drag.

$$C_N = C_{NL} \sin\beta \cos^2\beta + C_{NN} \left|\sin\beta\right| \sin\beta \qquad (1)$$

Coordinate Systems

The calculations for the circulatory lift on the hull are performed in a yawed earth-fixed frame with the x-axis aligned with the ship-fixed x-axis positive forward, the y axis parallel to the calm water surface positive to port, and the z-axis aligned with the earth-fixed Z axis positive up. The longitudinal origin is placed at the center of the instantaneous wetted length, the vertical origin is located at the waterline height of the section where the maximum draft is located and the transverse position is aligned with CG of the ship. This is illustrated in Fig. 1 for a ship in calm water and in Fig. 2for a ship operating in waves.

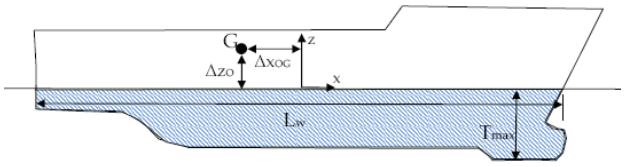

Fig.1: Yawed earth-fixed frame for an upright ship in calm water.

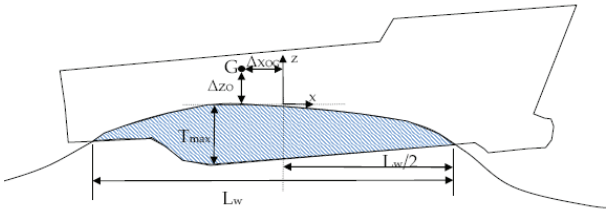

Fig.2: Yawed earth-fixed frame for a ship in waves.

For the 2D sectional calculations, it is useful to define the geometry of a hull section having arbitrary motion in the presence of waves, as illustrated in Fig. 3. In the case shown, the hull has a roll angle, ϕ, and local relative velocity vector, $\vec{V}_{rel}$, that is in the plane of the section. This vector includes the effects of the rigid body motions of the hull and makes an angle, α_v, relative to the horizontal plane. The instantaneous wave slope at the section is defined by the intersection of the water and the hull surface. The two intersection points, p_{i-1} and p_{i-2}, define the submerged shape of the section. The wave slope also defines an auxiliary wave slope coordinate system ($\tilde{X}, \tilde{Y}, \tilde{Z}$) in the plane of the section, centered at the midpoint of the chord of the submerged section. The angle between the wave slope system and the ship-fixed system is represented by the angle φ in Fig. 3. A separate auxiliary wave slope coordinate system is derived for each section at every time step.

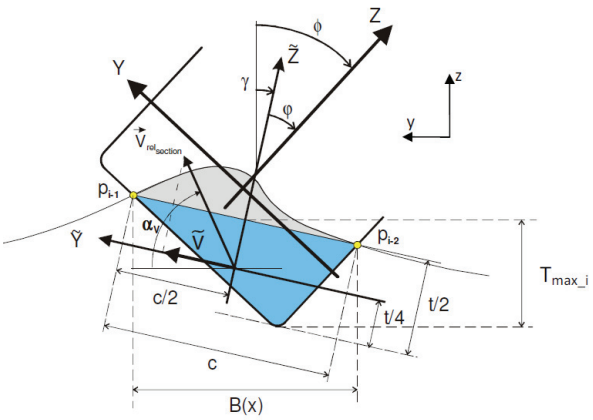

Fig.3: Wave slope frame for sectional calculations

LOW ASPECT RATIO WING THEORY

The circulation around the hull at a drift angle is analogous to the circulation of the flow about a low aspect ratio wing. The lift on the hull resulting from this circulation can be modeled by treating the submerged portion of the ship as a low aspect ratio foil, where the wetted length of the hull is the chord length and the maximum instantaneous draft is the span of the airfoil. Jones (1946) developed the expressions shown in Eqn. (2) for the linear lift and drag on a low aspect ratio delta wing at a small angle of attack, α, where a_e is the effective aspect ratio that for a ship includes the wall effect of the free surface and is defined in Eqn. (3).

$$C_L = \frac{\pi}{2} a_e \alpha \quad , \quad C_D = \frac{C_L^2}{\pi a_e} \tag{2}$$

$$a_e = \frac{2T_{\max}}{L_W} \tag{3}$$

The lift and drag coefficients in Eqn. (2) are "tuned" to match the linear terms corresponding to drift and yaw rate (Y_v, K_v, N_v, Y_r, N_r, and K_r) from a traditional calm water maneuvering model of the form developed by Abkowitz (1969). The tuning can be performed at a range of Froude numbers to include the influence of Froude number on the bare hull forces. The effect of the Munk moment will be accounted for in the tuned linear lift coefficients, so it is important to remove terms corresponding to the Munk moment from the hydrodynamic disturbance force model in Tempest. The dimensional linear normal force on the hull in the yawed earth-fixed frame from the drift angle and yaw rate is computed using Eqn. (4). The speed dependent tuning coefficients defined in Eqn. (5), C_{Nv}^L and C_{Nr}^L, are added to match the empirical data for the upright ship in calm water.

$$F_N^L = F_{Nv}^L + F_{Nr}^L \qquad \text{where,}$$

$$F_{Nv}^L = C_{Nv}^L(Fn)\frac{\pi}{2} a_e \sin\beta\left(\tfrac{1}{2}\rho U^2 LT\right)\cos^2\beta$$

$$F_{Nr}^L = C_{Nr}^L(Fn)\frac{\pi}{4} a_e \frac{\tilde{r}L}{U}\left(\tfrac{1}{2}\rho U^2 LT\right)\cos^2\beta \tag{4}$$

where,

$$C_{Nv}^L(Fn) = -\frac{Y_v(Fn)L_{W\_calm}}{\pi/2\, a_e T_{\max\_calm}}$$

$$C_{Nr}^L(Fn) = \frac{Y_r(Fn)L_{W\_calm}}{\pi/4\, a_e T_{\max\_calm}} \tag{5}$$

The calculations are performed in the yawed earth-fixed frame, so the drift angle and yaw rate should be defined in this frame. $\tilde{r}$ is the rotational velocity about the yawed earth-fixed z-axis. The local drift angle and local lateral plane velocity will first be computed at each section specified for the cross-flow drag calculations. The overall drift angle, β, and lateral velocity, U, used in Eqn. (4) will then be obtained by averaging over the sections. The velocity U includes the velocity from the ship body motion and the longitudinal component of the wave orbital velocity. Only the (ship-fixed) longitudinal component of the ambient wave orbital velocity is included because the contribution to the total fluid velocity due to radiation and diffraction cannot be obtained within the current hydrodynamic framework in Tempest. Including the ambient wave velocity in the absence of the disturbance (radiation and diffraction) velocity would provide a higher velocity than reality in the transverse plane, which has strong effects on the hull forces due to the quadratic effect of the velocity on the force.

However, because the disturbance velocity is assumed to be small in the longitudinal direction for slender ships, the orbital velocity is included in this direction. The $\cos^2\beta$ factor in Eqn. (4) follows the method from Hooft (1994) where the force from the drift angle is normalized using the square of the axial component of the velocity. The $\cos^2\beta$ factor also has the advantage that it results in a maximum normal force at about 40°, which is a reasonable estimate for the stall angle, and causes the normal force to go to zero at a drift angle of 90°. With this behavior there is no need for an empirical stall model to be included. The values for L, T and ae in Equation (4) are the instantaneous wetted length and maximum draft, which are shown as L_W and T_{max} in Fig. 1, and the effective aspect ratio computed from those values for L and T using Eqn. (3). The values for L, T and a_e used to compute the tuning coefficients in Equation 5. are based on the initial calm water geometry as shown in Fig. 1.

The value of the maximum draft in the yawed earth fixed frame is not obvious for sections with a roll angle in waves. The maximum draft at each section is computed as the vertical distance in the earth-fixed frame between the average waterline height and the deepest point on the section as shown in Fig. 3. The overall maximum draft (T_{max}) is defined as the largest value of T_{max_i} over all the sections defining the hull.

In addition to computing the side force acting on the hull the yaw and roll moment from the lift on the hull must be computed. The moments about the yawed earth-fixed z-axis and x-axis are computed by multiplying the computed normal force by a moment arm. The appropriate moment arm is determined from the linear derivatives for the yaw and roll moment in calm water, with the assumption that the distance from the center of pressure to the origin as a percentage of the wetted length and maximum draft remains constant as the ship maneuvers in waves. The formula for computing the moment about the yawed earth-fixed z-axis is given in Eqn. (6).

$$M_Z^L = F_{Nv}^L C_{Mv}^L(Fn) L_W + F_{Nr}^L C_{Mr}^L(Fn) L_W \tag{6}$$

where,

$$C_{Mv}^L(Fn) = \frac{N_v(Fn)}{Y_v(Fn)};\ C_{Mr}^L(Fn)\frac{N_r(Fn)}{Y_r(Fn)} \tag{7}$$

The formula for computing the moment about the yawed earth-fixed x-axis is:

$$M_X^L = F_{Nv}^{LK} C_{Kv}^L(Fn) T_{\max} + F_{Nr}^{LK} C_{Kr}^L(Fn) T_{\max} \tag{8}$$

where,

$$C_{Kv}^L(Fn) = \frac{K_v(Fn) L_{W\_calm}}{Y_v(Fn) T_{\max\_calm}};$$
$$C_{Kr}^L(Fn) = \frac{K_r(Fn) L_{W\_calm}}{Y_r(Fn) T_{\max\_calm}} \tag{9}$$

The linear normal forces used to compute the roll moment, F_{Nv}^{LK} and F_{Nr}^{LK}, are adjusted to remove the influence of the roll velocity on the normal force in order to avoid double counting of the roll moment computed from a separate roll damping model in Tempest, which computes a roll moment proportional to roll velocity. C_{Mv}^L and C_{Mr}^L represent the longitudinal position of the center of pressure of the normal force due to drift angle and turning as a percentage of the instantaneous wetted length. C_{Kv}^L and C_{Kr}^L represent the vertical position of the center of pressure of the normal force due to drift angle and turning as a percentage of the instantaneous maximum draft. Equations (6) and (8) compute the moment about the yawed-earth fixed frame referenced to the origin of that frame. To reference these moments to the center of gravity of the ship the moment arms are adjusted to account for the distance from the origin of the yawed earth-fixed frame to the center of gravity, which are shown as Δz_{OG} and Δx_{OG} in Fig. 2, representing the shift in the yawed earth-fixed z and x directions. Adding these values to Equations (6) and (8), the moments in the yawed-earth fixed frame referenced to the center of gravity are defined as:

$$M_{Z\_G}^L = F_{Nv}^L\left(C_{Mv}^L(Fn) L_W + \Delta z_{OG}\right) + F_{Nr}^L\left(C_{Mr}^L(Fn) L_W + \Delta z_{OG}\right) \tag{10}$$

$$M_{X\_G}^L = F_{Nv}^{LK}\left(C_{Kv}^L(Fn) T_{\max} - \Delta x_{OG}\right) + F_{Nr}^{LK}\left(C_{Kr}^L(Fn) T_{\max} - \Delta x_{OG}\right) \tag{11}$$

where Δz_{OG} is positive if the center of gravity is above the origin and Δx_{OG} is positive if center of gravity is forward of the origin.

A force in the yawed-earth fixed x direction from the induced drag is also included. The induced drag on a low aspect ratio foil is related to the circulatory lift by Jones (1946) using the second formula listed in Equation (2). In this case the normal force will be used instead of the lift force and tuning coefficients will be included to calibrate with empirical data for the additional drag measured during steady drift and turning. It is assumed that this force can be applied at the ship center of gravity, and therefore does not contribute to the moments about the center of gravity. The induced drag force in the yawed earth-fixed x-direction is computed as:

$$F_X^L = F_{Xv}^L + F_{Xr}^L \qquad \text{where,}$$

$$F_{Xv}^L = C_{Xv}^L(Fn)\frac{\pi}{4}a_e \sin^2\beta\left(\tfrac{1}{2}\rho U^2 LT\right)\cos^2\beta \qquad (12)$$

$$F_{Xr}^L = C_{Xr}^L(Fn)\frac{\pi}{16}a_e\left(\frac{\tilde{r}L}{U}\right)^2\left(\tfrac{1}{2}\rho U^2 LT\right)\cos^2\beta$$

The tuning coefficients are determined in this case from the quadratic coefficients X_{vv} and X_{rr} :

$$C_{Xv}^L(Fn) = \frac{X_{vv}(Fn)L_{W\_calm}}{\tfrac{\pi}{4}a_e T_{\max\_calm}};$$

$$C_{Xr}^L(Fn) = \frac{X_{rr}(Fn)L_{W\_calm}}{\tfrac{\pi}{16}a_e T_{\max\_calm}} \qquad (13)$$

Input for X_{vv} and X_{rr} should both have negative values, since they are defined with a coordinate system with x forwards. All the forces and moments computed from the hull circulatory lift and drag model are computed first in the yawed earth-fixed frame, but are transformed to the ship-fixed frame before they are added to the other component forces and moments within the Tempest framework.

CROSS-FLOW DRAG MODEL

At higher drift angles, cross-flow drag becomes the dominant viscous effect on the hull. The cross-flow drag force is obtained by first dividing the hull into a series of 2D sections. The local cross flow drag at each section is computed, and then the total cross-flow drag force is obtained by integrating the sectional forces along the length of the hull. The 2D sectional cross-flow drag calculations are performed in the local wave-slope frame for each section that was described earlier and is depicted in Fig. 3. The cross-flow drag force on each section is computed from the local cross flow velocity at the section and a drag coefficient, $C_d(x,Re)$, which is dependent on the shape of the section as well as the Reynolds number at the section. The local cross-flow velocity is taken as the velocity component parallel to $\tilde{Y}$ axis of the wave-slope frame, and is depicted as $\tilde{v}$ in Fig. 3 and 4. The relative velocity used for the maneuvering calculations on each section will be computed at the center of the bounding box surrounding the section. This velocity includes the coupled effects of rigid body motions in 6 degrees of freedom. Since the transverse and vertical components of ambient wave orbital velocity are ignored in the present implementation of this cross-flow drag model, the sectional velocity in the y-z plane will only be due to rigid body motions. The section shapes used for the cross-flow drag calculations are obtained by reflecting the instantaneous wetted geometry about the approximated wave-slope line as shown in Fig. 4.

Two methods are available for obtaining the cross-flow drag coefficient $C_d(x, Re)$ for each section. In the first option, the instantaneous beam to draft ratio of the section is used to estimate $C_d(x, Re)$ based on wind tunnel data for elliptical or rectangular shaped cylinders. In the second option the user specifies the values for $C_d(x, Re)$ for each section at a range of heel angles and drafts, and the value at each time step for each section is then obtained through interpolation based on the instantaneous draft and roll angle relative to the wave slope frame. It is possible to use the second option for some sections and the first option for the other sections. Such an approach may be useful in the case of a ship with a large skeg, where the user could specify the coefficients directly for sections with the skeg, but use the first option on the sections forward of the skeg.

Hoerner (1965) provides a general discussion of sectional drag and shows the behavior of the drag coefficient for various sectional 2D shapes in steady flow. These shapes

include parametrically varied rectangular, elliptic, and u/v shapes that are somewhat like ship hull section shapes. The data in Hoerner show that the dependence of the 2D cross-flow drag coefficient on Reynolds number is primarily a step function at the critical Reynolds number where the flow transitions from laminar to turbulent flow. For full-scale simulations the flow will be turbulent, but for model-scale simulations laminar flow may be present on some sections. Based on the data in Hoerner (1965), approximate curves for $C_d(x, Re)$ were generated for elliptical sections and rectangular sections with a moderate bilge radius. These curves are shown in Fig. 5 and are used to compute $C_d(x, Re)$ in the current method. The cross-flow drag coefficient is dependent on the instantaneous thickness and chord of the section, which are indicated by t and c respectively in Fig. 4 as well as whether the section shape more closely resembles an ellipse or a rectangle with rounded corners

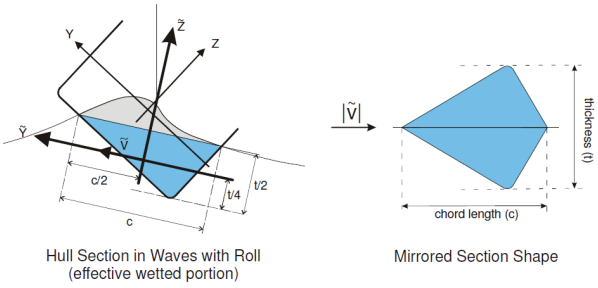

Fig. 4: Mirrored section shape used for 2D cross-flow drag calculations.

.

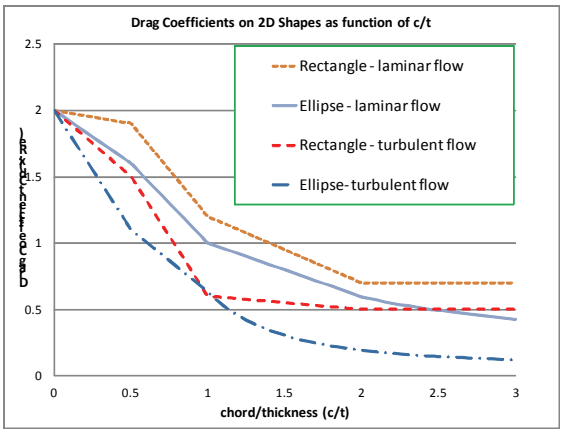

Fig.5: Cd(x,Re) for elliptical and rectangular sections as a function of c/t, in laminar and turbulent flow.

The general equations for the ship fixed reference frame sway and heave forces and yaw and pitch moments from the cross-flow drag model, adjusted for the presence of waves and ship motions are given by Equations (14) through (17). There is no surge force component from the cross-flow drag model.

$$F^{cf}_{Y\_G} = -\frac{\rho}{4}\int_0^L t(x)\, C_d(x,\mathrm{Re})\, \tilde{v}(x)\left|\tilde{v}(x)\right|\cos\varphi(x)\, dx \qquad (14)$$

$$F^{cf}_{Z\_G} = -\frac{\rho}{4}\int_0^L t(x)\, C_d(x,\mathrm{Re})\, \tilde{v}(x)\left|\tilde{v}(x)\right|\sin\varphi(x)\, dx \qquad (15)$$

$$M^{cf}_{Z\_G} = -\frac{\rho}{4}\int_0^L t(x)\, C_d(x,\mathrm{Re})\, \tilde{v}(x)\left|\tilde{v}(x)\right|\cos\varphi(x)\, x\, dx \qquad (16)$$

$$M^{cf}_{Y\_G} = \frac{\rho}{4}\int_0^L t(x)\, C_d(x,\mathrm{Re})\, \tilde{v}(x)\left|\tilde{v}(x)\right|\sin\varphi(x)\, x\, dx \qquad (17)$$

The cos φ(x) and sin φ(x) terms appearing in the above equations provides the transformation of the sectional drag force back to the ship fixed coordinate system from the local $\tilde{Y}\tilde{Z}$ coordinate system. When applying Equations (14) through (17), the variable x must be defined in the ship-fixed frame.

There is also a roll moment generated by the ship-fixed sway force calculated above ($F^{cf}_{Y\_G}$). Initially it will be assumed that the force is evenly distributed along the $\tilde{Z}$ axis. With this assumption the moment arm will act at 50% of the distance from the water surface to the half thickness (t/2) of the section, so the default value of zcp(x,Re) is 0.5. It is suggested that RANS computations be performed on a variety of sections to obtain better estimates of the moment arm. With the current assumptions, the roll moment is:

$$M^{cf}_{X\_G} = -\frac{\rho}{4}\int_0^L t(x)\left[z_{cp}(x,\mathrm{Re})\frac{t(x)}{2} + \tilde{z}_{cg}\right] C_d(x,\mathrm{Re})\, \tilde{v}(x)\left|\tilde{v}(x)\right|\cos\varphi(x)\, dx \qquad (18)$$

where $\tilde{z}_{cg}$ is the distance in the direction of the $\tilde{Z}$ axis from the projection of the center of gravity onto the section plane to the instantaneous

waterline defined in the $\tilde{Y}\tilde{Z}$ system (the line connecting p_{i-1} and p_{i-2} in Fig. 3). $\tilde{z}_{cg}$ is positive when the CG is above the waterline.

Longitudinal attenuation of cross-flow drag

Equations (4) through **12)** define the forces and moments from circulatory lift in the yawed earth-fixed frame. These forces are transformed to the ship-fixed frame and added to the forces and moments due to cross-flow drag, defined in Equations (14) through **(18)**, to obtain the total hull lift and cross-flow drag forces and moments in the ship-fixed frame at each time step. Built into the models is a natural implied blending of the low aspect ratio airfoil forces and those from cross-flow drag. As the cross-flow drag force is roughly proportional to $\sin^2\beta$, the cross-flow drag force will be very small at low drift angles. It has been found through experiments, that at low and moderate drift angles, the distribution of cross flow drag force is such that this force acts mainly on the aft portion of the ship (see Hooft, 1994). An attenuation factor is applied to the cross flow drag coefficients at each section to reduce their value on the forward portion of the ship at low drift angles. As the drift angle increases the attenuation is diminished. Fig. 6, taken from Hooft (1994) shows a schematic of the attenuation factor for a range of drift angles. The schematic is based on segmented model test data for a Series 60 hull; however, the model tests were performed only up to a drift angle of 20˚. The curves shown for drift angles higher are based on extrapolation. At 90˚ drift there will be no attenuation and at drift angles higher than 90˚ the attenuation will be such that the cross-flow drag force will be shifted towards the forward portion of the ship. CFD analysis can be performed to produce curves of the attenuation factor along the length of the hull at various drift angles, and then interpolation can be used to obtain the attenuation factor at each section at the current drift angle during the simulation. The attenuation factor, $C_{T\text{-}Cd}(x,\beta)$, is used to determine a corrected cross-flow drag coefficient, C_{d_corr}.

$$C_{d\_corr}(x,\mathrm{Re},\beta) = C_{T-Cd}(x,\beta)\, C_d(x,\mathrm{Re}) \qquad (19)$$

The corrected coefficient, $C_{d\_corr}(x,\mathrm{Re},\beta)$, is used in place of $C_d(x,\mathrm{Re})$ in Equations (14) through (18).

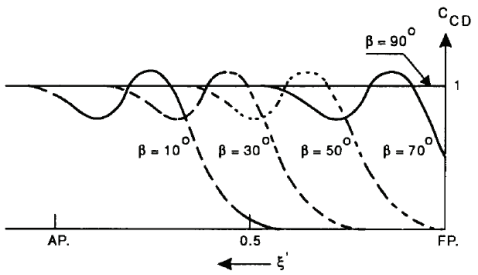

Fig. 6: Schematic indication of the longitudinal attenuation of Cd(x,Re) as a function of drift angle, from Hooft (1994).

SAMPLE CALCULATION

The hull lift and cross-flow drag model has been implemented into the Tempest code and some preliminary calculations have been performed for the pre-contract DDG-51 hull form as represented by NSWCCD model 5415. The preliminary simulations have been performed using an approximate attenuation factor, $C_{T\text{-}Cd}(x,\beta)$, based on the limited Series 60 model test results discussed in Hooft (1994). For future simulations, RANS calculations will be performed to compute the attenuation factor. The RANS simulations will be performed over a large range of drift angles, with the results analyzed to provide the longitudinal distribution of the forces along the length of the hull in addition to the total forces. The simulations were not completed in time to compute attenuation factors for the computations show in this paper. Results from some of the RANS simulations that have been completed have led to some new insights. For instance it is apparent that to predict the roll moment for some hull forms the model will need to include vertical component of forces (heave and pitch) in addition to lateral plane forces.

Results from the preliminary simulations performed in calm water have been compared with PMM model test results performed at the University of Iowa (Yoon 2009) and free running model tests performed at NSWCCD (Hayden 2006). The comparisons with the PMM tests were performed with the model fixed at the calm water draft and trim in both the Tempest simulations and the model tests. The Tempest simulations were performed with and without the approximate attenuation factor switched on. Comparisons between the predictions and the

model test results are shown in Fig. 7 and Fig. 8 for the non-dimensional side force and yaw moment respectively for the model traveling at a steady drift angle. The approximate attenuation factor improves the comparison for the side force and the correlation for the side force is very good for this case. However, the inclusion of the attenuation factor degrades the correlation for the yaw moment. It is anticipated that this correlation will improve once ship specific attenuation factors based on the RANS simulations are incorporated. Fig 9 shows the comparison between the predictions and the data from free running model tests for the tactical turning diameter. Fig. 10 compares the steady heel angle in a turn for the same model tests. In both cases the correlation is good and falls within the scatter of the model test data.

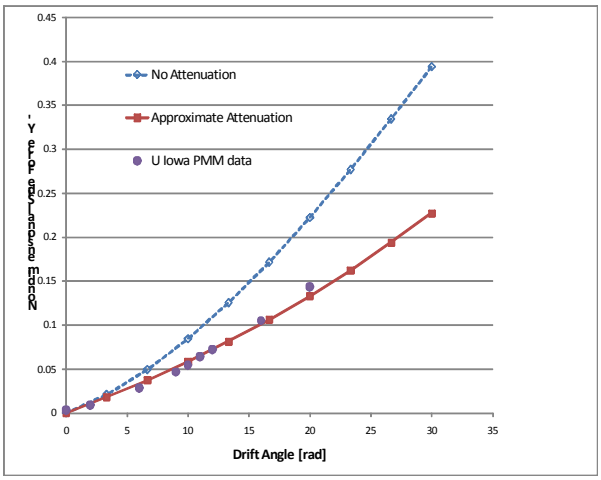

Fig. 7: Comparison of non-dimensional side force on the pre-contract DDG-51 at Fn=0.28.

CONCLUSIONS

A model has been developed which computes the hull lift and cross-flow separation forces on a ship maneuvering in waves. The model is computationally efficient and accounts for the changing wetted geometry of the ship hull, while retaining the ability to be calibrated to match available calm water maneuvering data. The model remains well behaved even at extreme drift angles and yaw rates as a ship may encounter during broaching. Preliminary calculations show the model predictions compared reasonably well with calm water model test results.

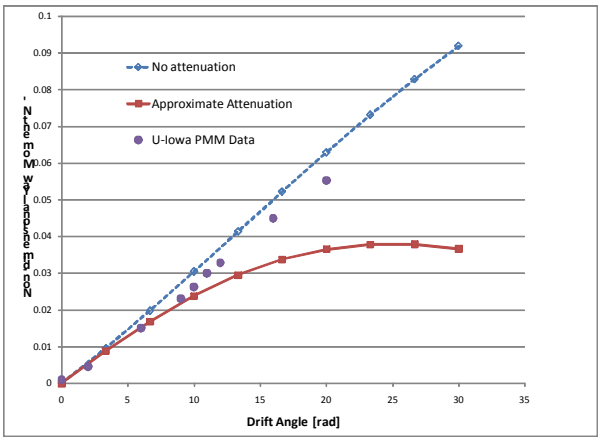

Fig.8: Comparison of non-dimensional yaw moment on the pre-contract DDG-51 at Fn=0.28.

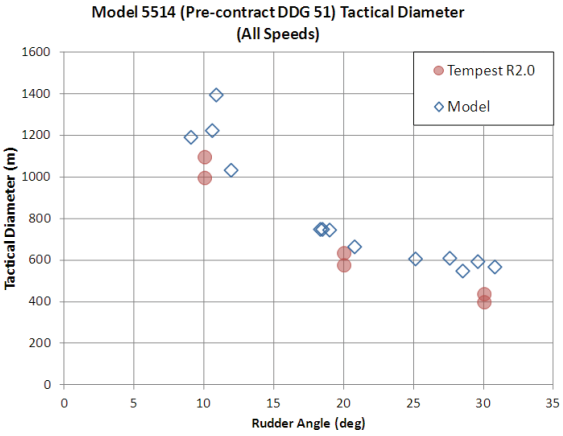

Fig.9: Comparison of tactical turning diameter on the pre-contract DDG-51 versus rudder angle.

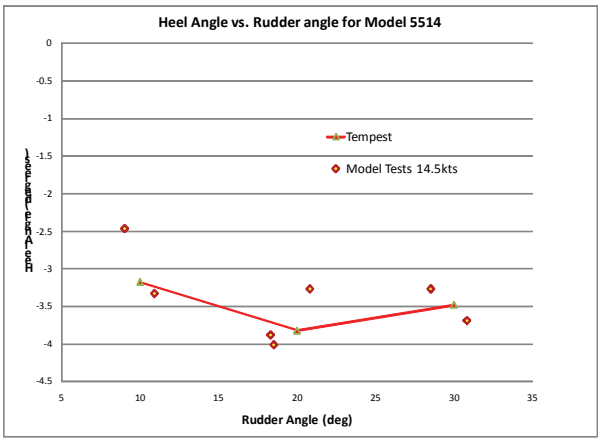

Fig.10: Comparison of steady heel angle in a turn for the pre-contract DDG-51 versus rudder angle, 14.5 knots full-scale.

ACKNOWLEDMENTS

Dr. Pat Purtell (ONR) and Jim Webster (NAVSEA) have supported the work discussed in this paper.

REFERENCES

Abkowitz, M. (1969), Stability and Motion Control of Ocean Vehicles, The MIT Press.

Belknap, W.F. and Reed, A.M. (2010), "TEMPEST – New Computationally Efficient Dynamic Stability Prediction Tool", Proc. of 11th Intl Ship Stability Workshop, Wageningen, the Netherlands

Greeley, D.S. (2011), "Some Results from a New Time-Domain Bilge keel Force Model", Proc. of 12th Intl Ship Stability Workshop, Washington DC.

Hayden, D.D., Bishop, R.C., Park, J.T. and Laverty, S.M. (2006), Model 5514 Capsize Experiiments Representing the Pre-Contract DDG51 Hull Form at End of Service Life Conditions, NSWCCD-50-TR-2006/020

Hoerner, S.F. (1965), Fluid Dynamic Drag: Theoretical, Experimental and Statistical Information, Hoerner Fluid Dynamics.

Hooft, J. P. and Nienhuis (1994), "The Prediction of the Ship's Maneuverability in the Design Stage," SNAME Trans Vol 102, pp 419-445.

Hughes, et. al. (2011) Tempest Release 2.2 Theory Manual, NSWCCD Report (in preparation)

Jones, R.T. (1946) Properties of Low-Aspect-Ratio Pointed Wings at Speeds Below and Above the Speed of Sound, NACA Report No. 835

Ross, A. (2008), "Nonlinear Manoeuvering Models for Ships: a Lagrangian Approach," PhD Thesis 2008:114.

Yoon, H. (2009), "Phase-averaged Stereo-PIV Flow Field and Force/Moment/Motion Measurements for Surface Combatant in PMM Maneuvers," Ph.D. thesis, The University of Iowa, Iowa City